Supporting Information: Investigating Closed and Open Site Stability of Sn-, Ti-, Zr-, and Hf-Beta Zeolites: A Comprehensive Periodic-DFT Study

Nawras Abidi, Yacine Boudjema, Céline Chizallet, and Kim Larmier*

IFP Energies nouvelles, Rond-point de l'échangeur de Solaize, 69360 Solaize, France

E-mail: kim.larmier@ifpen.fr

Table S1: Number of valence electrons in our calculations: Data from POTCAR files

Element	**Number of valence Electrons**
Hydrogen (H)	1
Carbon (C)	4
Nitrogen (N)	5
Oxygen (O)	6
Silicon (Si)	4
Tin (Sn)	14
Titanium (Ti)	12
Zirconium (Zr)	12
Hafnium (Hf)	12

Table S2: Unit cell parameters for different metal substitutions in the different T-sites of zeolite Beta

T Site-Metal	a (Å)	b (Å)	c (Å)	α (°)	β (°)	γ (°)
T1-Sn	17.80	17.84	14.58	90.1	114.7	90.2
T1-Ti	17.81	17.82	14.60	90.1	114.8	90.2
T1-Zr	17.82	17.83	14.55	90.3	114.6	90.3
T1-Hf	17.83	17.83	14.55	90.2	114.6	90.2
T6-Sn	17.78	17.88	14.54	90.1	114.7	90.4
T6-Ti	17.78	17.88	14.57	90.1	114.7	90.5
T6-Zr	17.79	17.90	14.49	90.1	114.5	90.6
T6-Hf	17.78	17.90	14.48	90.1	114.5	90.5
T9-Sn	17.79	17.77	14.54	90.0	114.5	90.0
T9-Ti	17.81	17.79	14.54	90.0	114.4	90.0
T9-Zr	17.82	17.78	14.52	90.0	114.3	90.0
T9-Hf	17.81	17.78	14.51	90.0	114.3	90.0

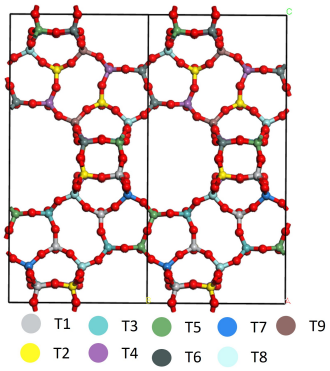

Parameter	Value
a (Å)	12.66
b (Å)	12.66
c (Å)	26.41
Alpha (°)	90.0
Beta (°)	90.0
Gamma (°)	90.0

Figure S1: Identification of T sites in Zeolite Beta, Polymorph A with the corresponding cell parameters based on the data in the International Zeolite association website.

Table S3: Comparative analysis of T sites in polymorphs A and B

Polymorph A	**Polymorph B**
T1	T2
T2	T1
T3	T6
T4	T5
T5	T4
T6	T3
T7	T9
T8	T8
T9	T7

Table S4: $\Delta_r E_{\text{ads}}(H_2O)$ of the first water molecule on different T sites with different metals for the zeolite (energies in kJ mol^{-1}).

T Site-Metal	**non-dissociated H_2O**	**Dissociated H_2O trans**	**Dissociated H_2O Syn**
T1-Sn	-65	-46	-41
T1-Ti	-38	-10	9
T1-Zr	-73	-32	-19
T1-Hf	-74	-31	-21
T6-Sn	-58	-36	-16
T6-Ti	-50	-12	6
T6-Zr	-73	-49	-20
T6-Hf	-92	-48	-24
T9-Sn	-76	-31	-13
T9-Ti	-50	3	5
T9-Zr	-79	-34	-17
T9-Hf	-85	-36	-24

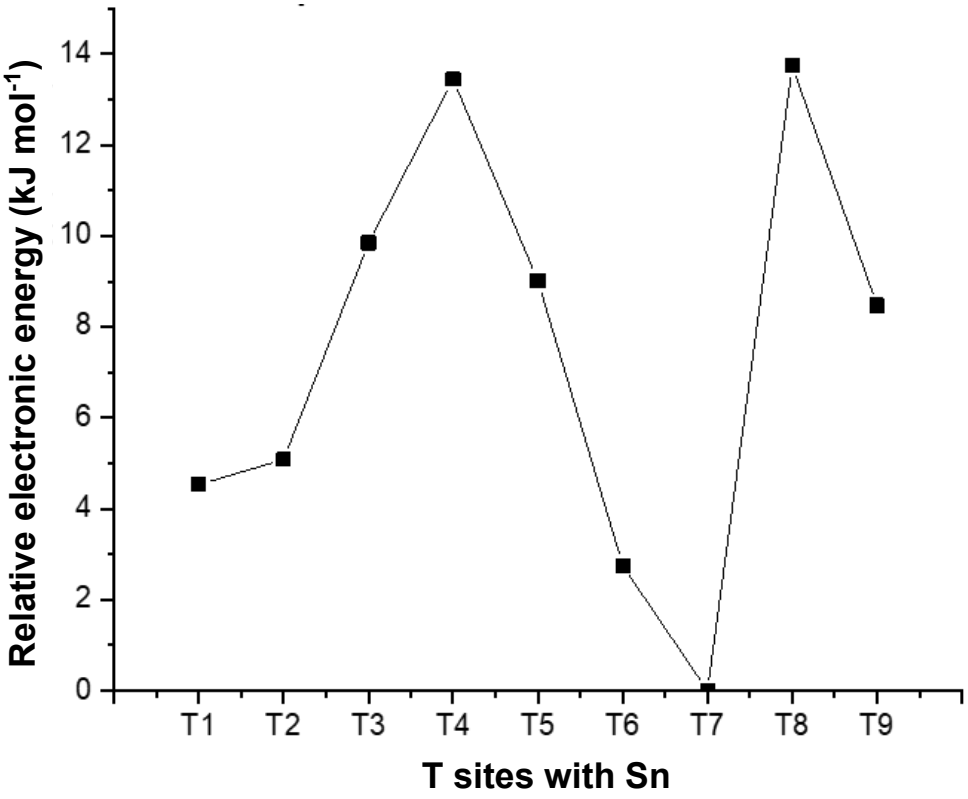

Figure S2: Relative electronic energy of the different T sites reported to the most stable one, in the case of Sn-Beta.

Table S5: $\Delta_r E_{\text{ads}}(H_2O)$ corresponding to the total electronic energy adsorption of n= 1 to 6 water molecules on different T sites with different metals of zeolite. The most stable energy is reported for each n water (energies in kJ mol^{-1}). The dispersion energy component is shown alongside the total energy for the adsorption of one water molecule.

T Site-Metal	**One H_2O (Total / Disp)**	**Two H_2O**	**Three H_2O**	**Four H_2O**	**Five H_2O**	**Six H_2O**
T1-Sn	-65 / -21	-98	-172	-189	-255	-300
T1-Ti	-38 / -21	-65	-115	-126	-130	-157
T1-Zr	-73 / -23	-97	-181	-199	-222	-251
T1-Hf	-74 / -24	-100	-181	-190	-196	-243
T6-Sn	-58 / -20	-104	-158	-231	-244	-303
T6-Ti	-50 / -17	-70	28	-144	-158	-261
T6-Zr	-73 / -13	-128	-189	-229	-248	-314
T6-Hf	-92 / -20	-154	-178	-215	-249	-314
T9-Sn	-76 / -23	-129	-178	-200	-240	-302
T9-Ti	-50 / -22	-86	-104	-150	-158	-192
T9-Zr	-79 / -22	-141	-174	-229	-245	-278
T9-Hf	-85 / -23	-159	-181	-220	-269	-276

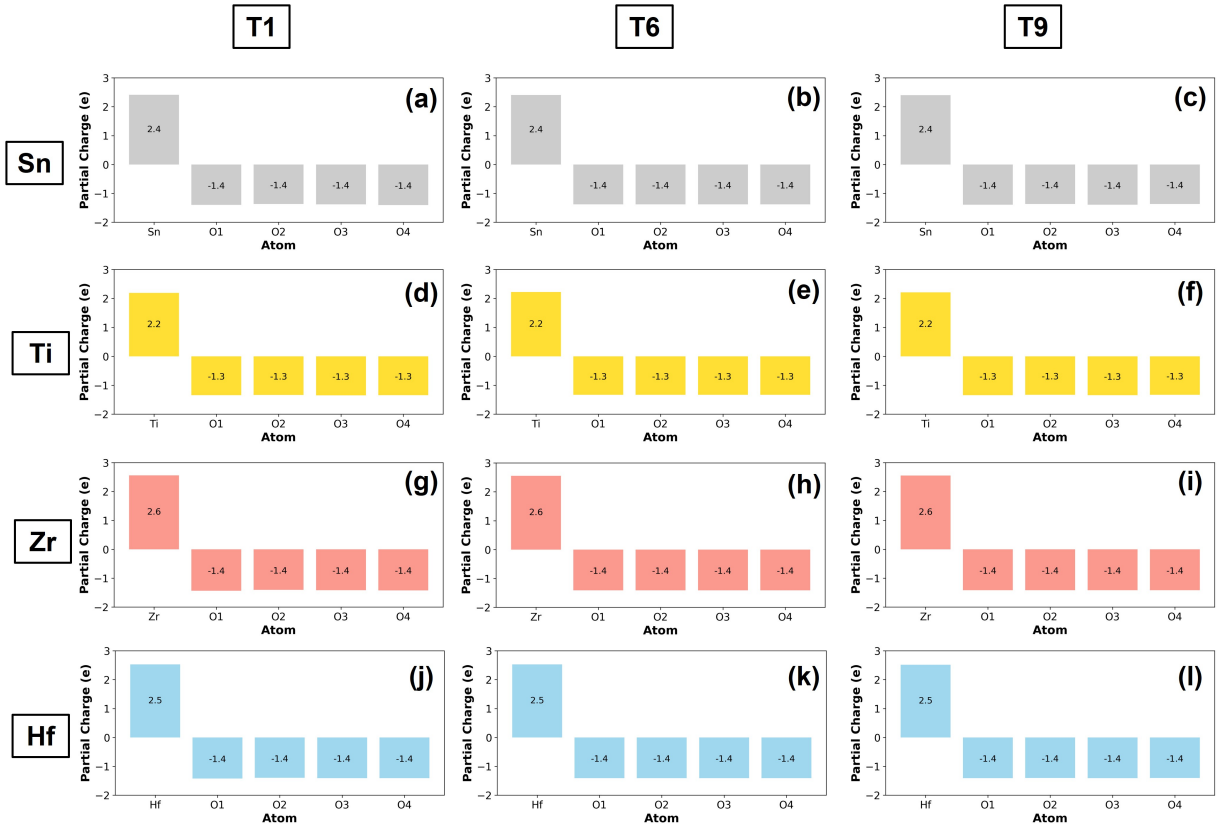

Figure S3: Bader charge distribution for various atoms across different T sites-Metals. Panels (a), (b), and (c) with grey color show the charge distribution for Sn at T1, T6, and T9, respectively. The yellow panels (d), (e), and (f) correspond to Ti, while the salmon panels (g), (h), and (i) depict Zr and the blue panels (j), (k), and (l) illustrate Hf. The values on the y-axis represent the Bader charge in elementary charge units (e), and the x-axis lists the atoms within the respective compounds. For reference, the Bader charges on Si atoms and O atoms bound only to Si atoms are of about +3.1 and -1.6, respectively.

Table S6: $\Delta_r G_{\text{ads}}(\text{Pyr})$ on the non-hydrated closed site, the hydrated site with non-dissociated water without water desorption, and the hydrated site with trans dissociated water for the different T sites with various metals in the zeolite (energies in kJ mol^{-1}) under pyridine pressure of 10^{-4} bar and a temperature of 298.15 K.

T Site-Metal	**Non-hydrated**	**Non-dissociated H_2O**	**trans dissociated H_2O**
T1-Sn	-60	-59	-86
T1-Ti	-20	-43	-42
T1-Zr	-58	-53	-74
T1-Hf	-64	-48	-81
T6-Sn	-76	-75	-59
T6-Ti	-29	-47	-26
T6-Zr	-66	-61	-58
T6-Hf	-75	-67	-67
T9-Sn	-43	-49	-86
T9-Ti	-15	-27	-57
T9-Zr	-39	-39	-70
T9-Hf	-59	-48	-70

Table S7: Standard Gibbs free energy of exchange ($\Delta_r G^{\circ}_{\text{exchange}}$, kJ mol^{-1}) for the hydrated closed-site with non-dissociated water of water exchange by pyridine for different T sites with various metals in the zeolite. Values are presented under standard conditions of a pyridine and water pressure of 1 bar and a temperature of 298.15 K.

T Site-Metal	**Non-dissociated H_2O**
T1-Sn	-78
T1-Ti	-55
T1-Zr	-58
T1-Hf	-57
T6-Sn	-89
T6-Ti	-50
T6-Zr	-55
T6-Hf	-60
T9-Sn	-50
T9-Ti	-48
T9-Zr	-41
T9-Hf	-55

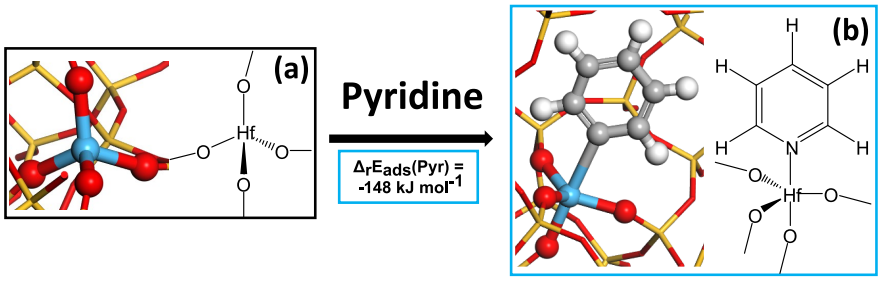

(i) Non-hydrated T1 site

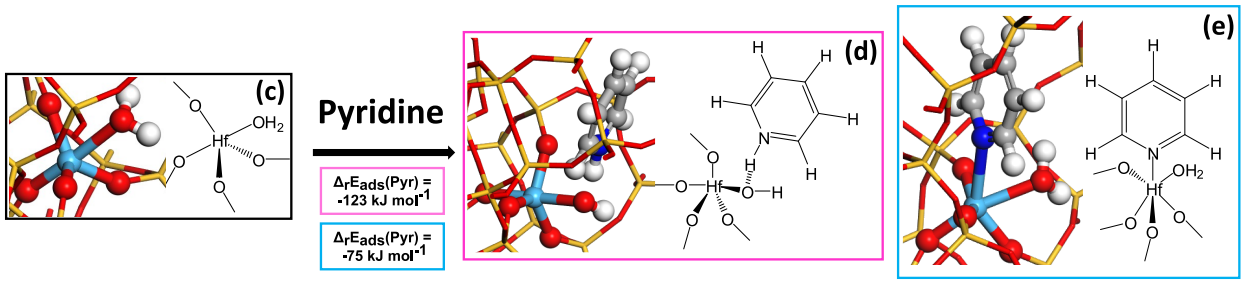

(ii) T1 site with a non-dissociated water molecule

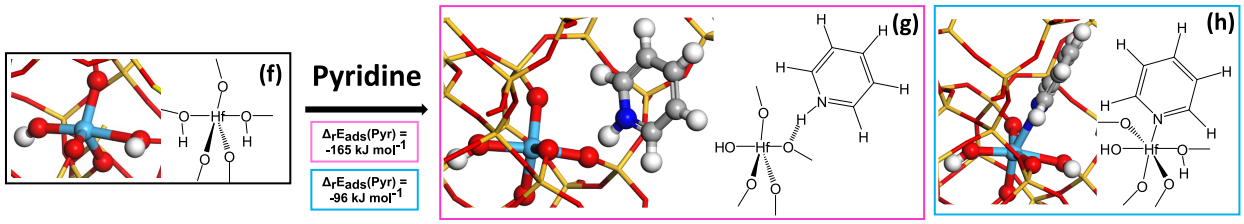

(iii) T1 site with a trans dissociated water molecule

Figure S4: Different tested adsorption modes of pyridine on different T1-Hf sites: (i) representing the non-hydrated T1 site, (ii) the T1 site with a coordinated non-dissociated water molecule, and (iii) the T1 site with a dissociated water molecule. The visualizations show pyridine interaction at the T1 sites with Hf, emphasizing the variations in molecular orientation and bonding configuration. The blue sky color refers to the Lewis acidity mode which is stable for the non-hydrated site. In presence of water, dissociated or not, it is very less stable compared to the Brønsted acidity mode indicated by the pink color. These results are the same for the other metals and T sites. The atom color coding is as follows: hydrogen (H) in white, carbon (C) in silver, nitrogen (N) in blue, oxygen (O) in red, silicon (Si) in yellow, and Hf in blue sky.

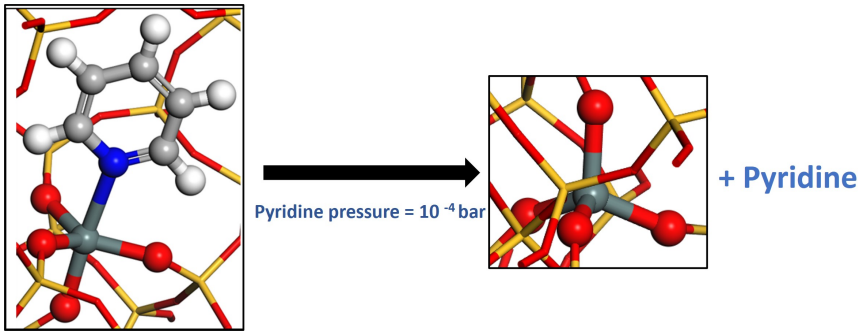

(i) Pyridine desorption on T1-Sn site

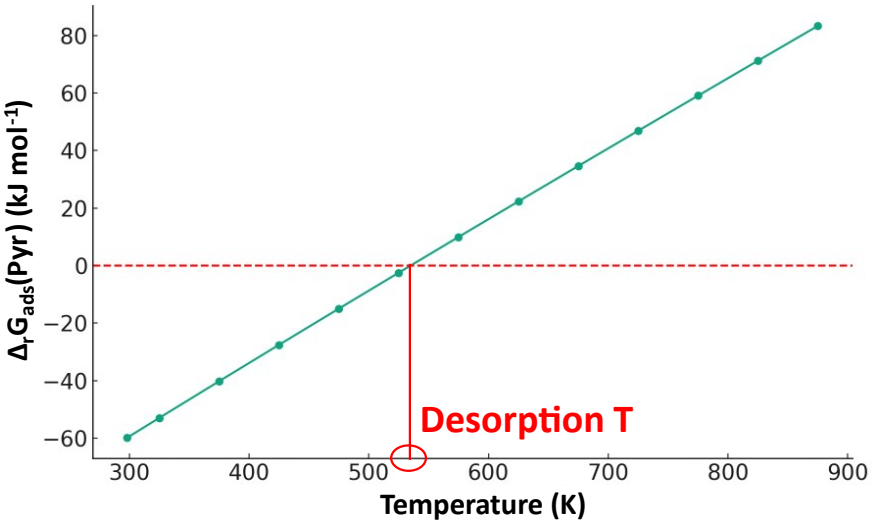

(ii) Desorption temperature graph

Figure S5: (i) Molecular simulation depicting the desorption of pyridine on a T1-Sn site within a zeolite framework at a pyridine pressure of 10^{-4} bar and (ii) graph showing the desorption temperature of pyridine, highlighted by the intersection of the extrapolated baseline (red dashed line) and the curve. This intersection point marks the significant desorption temperature of pyridine, as indicated by the red circle and "Desorption T" label. The atom color coding for the simulation is as follows: hydrogen (H) in white, carbon (C) in silver, nitrogen (N) in blue, oxygen (O) in red, Tin (Sn) in dark grey, and silicon (Si) in yellow.

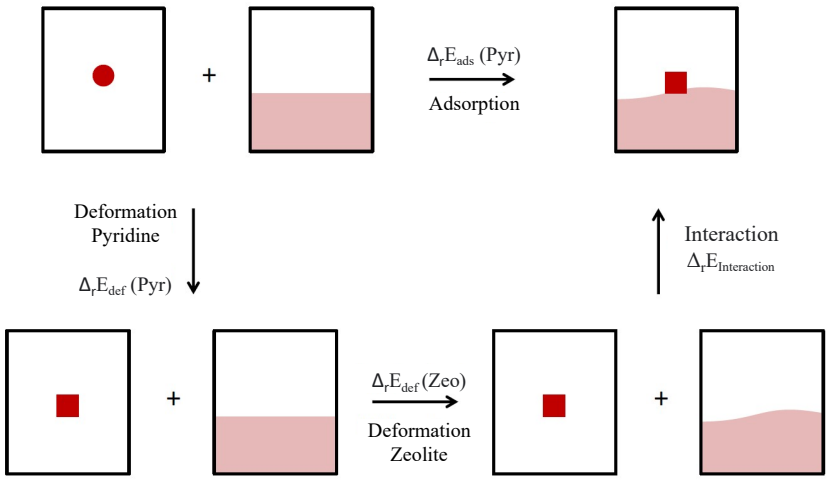

(i) Analysis of electronic adsorption energy components

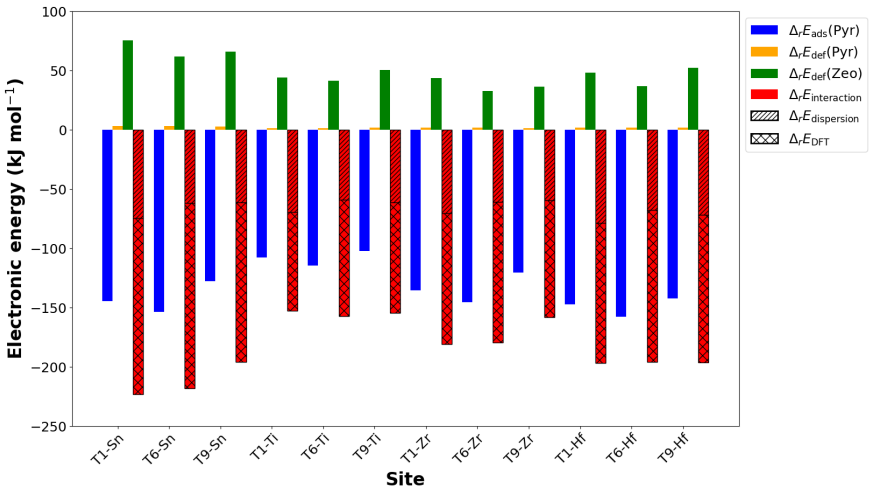

(ii) Electronic energy variation in pyridine adsorption at various catalytic sites

Figure S6: (i) Illustration of the methodology for computing different components of the electronic adsorption energy of pyridine. The circle represents pyridine before adsorption and deformation, and the square represents pyridine after these processes. The pink area denotes the zeolite surface, which also undergoes changes upon deformation and pyridine adsorption. (ii) Graph showing the adsorption energy of pyridine ($\Delta_r E_{\text{ads}}(\text{Pyr})$), deformation energy of pyridine ($\Delta_r E_{\text{def}}(\text{Pyr})$), deformation energy of the zeolite framework ($\Delta_r E_{\text{def}}(\text{Zeo})$), and interaction energy ($\Delta_r E_{\text{interaction}}$=$\Delta_r E_{\text{dispersion}}$+$\Delta_r E_{\text{DFT}}$) across various sites labeled T1, T6, and T9 with elements Sn, Ti, Zr, and Hf.

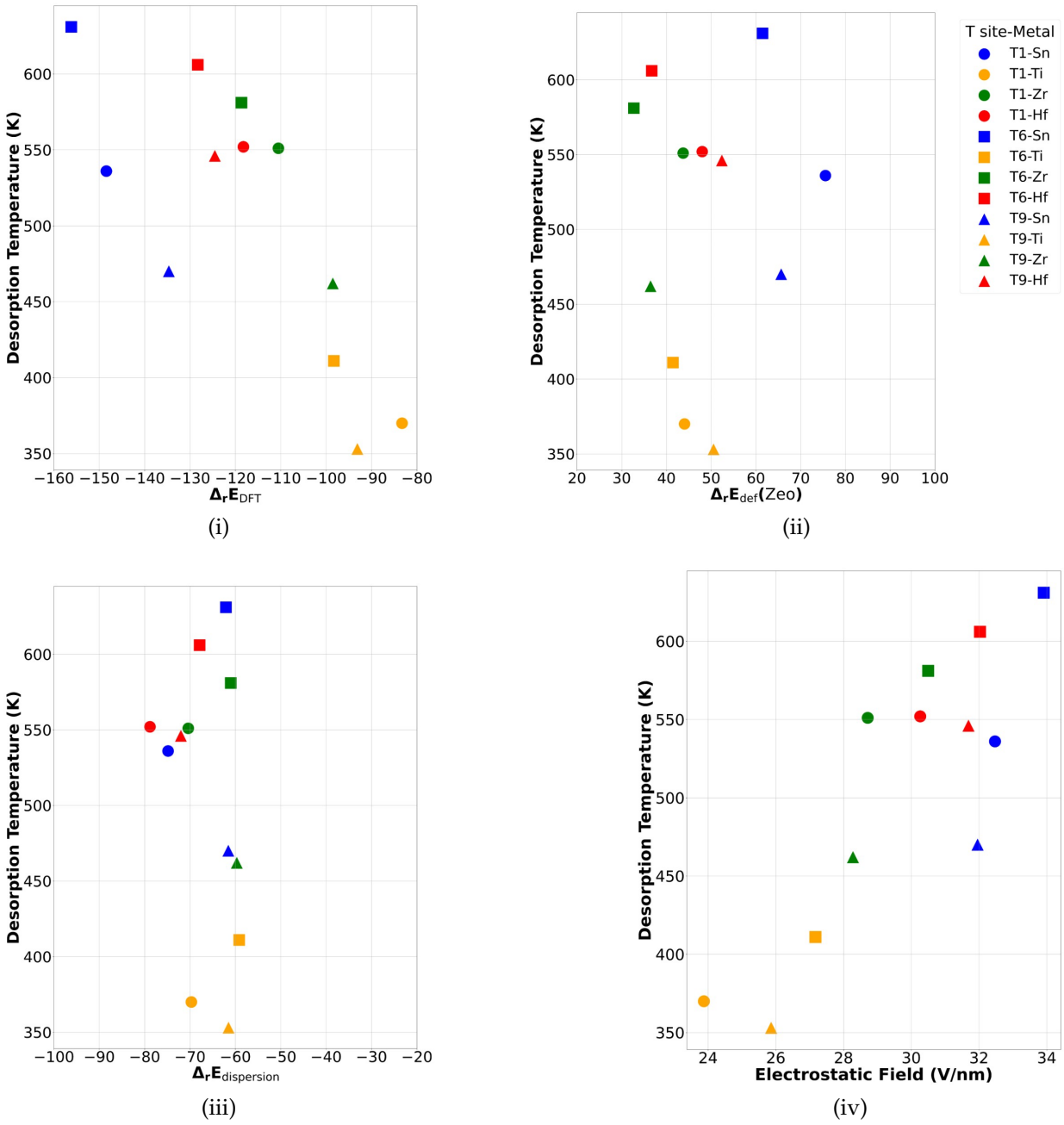

Figure S7: Comparative analysis of the desorption temperature (T) of pyridine as a function of different properties related to the pyridine adsorption across various T-Metal sites, all the energies are in kJ mol^{-1}: (i) relates T to the DFT electronic energy, $\Delta_r E_{\mathrm{DFT}}$, showcasing the electronic factors affecting pyridine desorption, (ii) illustrates the variation of T with respect to the energy of the deformation of the zeolite framework, $\Delta_r E_{\mathrm{def}}(\mathrm{Zeo})$, (iii) examines the impact of the dispersion part of the interaction energy, $\Delta_r E_{\mathrm{dispersion}}$, on T, and (iv) shows the relationship between T and the electrostatic field for different elements, indicating how the field influences desorption. Each sub-figure differentiates data points by the site-metal combination, providing a detailed breakdown of desorption behaviors.